



OPEN

Performance of a UV-A LED system for degradation of aflatoxins B₁ and M₁ in pure water: kinetics and cytotoxicity study

Judy Stanley¹, Ankit Patras¹✉, Brahmaiah Pendyala¹✉, Matthew J. Vergne² & Rishipal R. Bansode³

The efficacy of a UV-A light emitting diode system (LED) to reduce the concentrations of aflatoxin B₁, aflatoxin M₁ (AFB₁, AFM₁) in pure water was studied. This work investigates and reveals the kinetics and main mechanism(s) responsible for the destruction of aflatoxins in pure water and assesses the cytotoxicity in liver hepatocellular cells. Irradiation experiments were conducted using an LED system operating at 365 nm (monochromatic wave-length). Known concentrations of aflatoxins were spiked in water and irradiated at UV-A doses ranging from 0 to 1,200 mJ/cm². The concentration of AFB₁ and AFM₁ was determined by HPLC with fluorescence detection. LC–MS/MS product ion scans were used to identify and semi-quantify degraded products of AFB₁ and AFM₁. It was observed that UV-A irradiation significantly reduced aflatoxins in pure water. In comparison to control, at dose of 1,200 mJ/cm² UV-A irradiation reduced AFB₁ and AFM₁ concentrations by 70 ± 0.27 and 84 ± 1.95%, respectively. We hypothesize that the formation of reactive species initiated by UV-A light may have caused photolysis of AFB₁ and AFM₁ molecules in water. In cell culture studies, our results demonstrated that the increase of UV-A dosage decreased the aflatoxins-induced cytotoxicity in HepG2 cells, and no significant aflatoxin-induced cytotoxicity was observed at UV-A dose of 1,200 mJ/cm². Further results from this study will be used to compare aflatoxins detoxification kinetics and mechanisms involved in liquid foods such as milk and vegetable oils.

Filamentous fungi invading various feed crops produces toxic secondary metabolites called mycotoxins which possess a serious threat to consumer health¹. Aflatoxins are highly cytotoxic and carcinogenic secondary metabolites, produced predominantly by *Aspergillus flavus* and *Aspergillus parviticus*, especially in the tropical and subtropical regions as hot and humid climatic conditions are optimal for mold growth and toxin production^{2,3}. Aflatoxins are difuranocoumarin derivatives formed from the polyketide pathway and include a group of 17 aflatoxins, among which AFB₁ is the predominant and is highly toxic⁴. Aflatoxin contamination in animal feed results in their carry-over in foods of animal origin such as eggs and milk. The major AFB₁ metabolite in milk, AFM₁, is formed due to the action of hepatic cytochrome P450-dependent polysubstrate monooxygenase enzyme superfamily as a result of the hydroxylation of the fourth carbon of the terminal furan ring. In dairy cows, the biotransformation rate of AFB₁ to AFM₁ ranges from 0.3 to 6.2%^{5,6}.

Aflatoxins are detrimental upon ingestion, inhalation, and skin contact; and the consequences of aflatoxin infection are collectively called aflatoxicosis. The biotransformation of AFB₁ in liver results in the production of AFB₁-8,9-epoxide which is highly related to the incidence of hepatocellular carcinoma^{6,7}. The carcinogenicity of AFM₁ is approximately one-tenth of that of AFB₁. The International Agency for Research on Cancer in 1993 classified AFB₁ under Group 1 carcinogen and AFM₁ under group 2B carcinogen⁸; therefore, some international organizations have enacted stringent regulations to mitigate aflatoxin contamination in food and feed. The

¹Food Biosciences and Technology Program, Department of Agricultural and Environmental Sciences, College of Agriculture, Tennessee State University, Nashville, TN 37209, USA. ²Department of Pharmaceutical Sciences, Department of Chemistry and Biochemistry, Lipscomb University, Nashville, TN 37204, USA. ³Center for Excellence in Post-Harvest Technologies, North Carolina Research Campus, North Carolina Agricultural and Technical State University, Kannapolis 28081, NC, USA. ✉email: apatras@tnstate.edu; bpendyal@tnstate.edu

maximum residue limit (MRL) of aflatoxins for human consumption ranges from 4 to 30 $\mu\text{g}/\text{kg}$ ⁹. The European Union has the strictest standards, the AFB₁ level should not exceed 2 $\mu\text{g}/\text{kg}$ in edible oils and AFM₁ levels should not exceed 0.05 $\mu\text{g}/\text{kg}$ ⁹. The United States Food and Drug Administration specified maximum acceptable limits of 20 $\mu\text{g}/\text{kg}$ for total aflatoxins and 0.5 $\mu\text{g}/\text{kg}$ for AFM₁ in human food and milk^{9,10}.

Aflatoxin contamination in food and feed can be reduced by various processing methods. For example, aflatoxin contamination during growth and storage of grains can be reduced by employing various pre- and post-harvest technologies. Several aflatoxin decontamination methods include destruction by physical methods including heating at high temperatures; selective separation using adsorbents such as reduced graphene-oxide-gold nanoparticles¹¹; chemical modification using several acids, bases, and oxidizing agents; and biological decontamination using enzymes and fermentation¹. Despite their efficacy, each method presents certain challenges such as utilization of chemicals, adverse impacts on the nutritional and sensorial attributes of the food, and difficulties in scale-up, thereby limiting their use in food industry¹². Exploration of safe, cost-effective, and novel food processing technologies with an objective of achieving maximum inactivation of aflatoxins with minimal effect on the quality of food helps to address these challenges¹³. Examples of alternative innovative food processing technologies include electromagnetic irradiation, advanced-packaging materials, and dielectric heating¹. Pulsed light technology, which effectively degrades aflatoxins, utilizes broad spectra of white light, that includes ultra-violet, visible and infra-red¹⁴. Studies show that the light intensity and the UV spectrum greatly influence the degradation of aflatoxins more than the visible and infra-red spectrum¹⁵.

UV irradiation has been demonstrated in literature as an effective physical method to inactivate chemical contaminants, and micro-organisms through photolysis and DNA damage, respectively^{16–20}. This non-thermal technology is efficient in degrading aflatoxins because of their photosensitivity²¹. Dominant sources of UV treatment such as low pressure and medium pressure mercury lamps were used to degrade aflatoxins. In a study, 98% reduction of AFB₁ in water was observed at an UV dose of 4,880 mJ/cm^2 using a medium pressure UV lamp which emits irradiation between 200 and 360 nm wavelength¹⁶. Similarly, 100% reduction of AFB₁ in peanut oil was observed when UV intensity (220–400 nm) of 800 mJ/cm^2 was used for 30 min²². In a separate study, irradiation at 365 nm showed nearly 100% degradation of AFM₁ in milk after 60 min of exposure to 100 W lamp²³. As an alternative to mercury containing traditional UV lamps, alternative sources of UV light such as UV-LEDs and excimer lamps are being studied for their application in food industry as they have several advantages like mercury free, high energy efficiency, constant light intensity and prolonged lifetime^{24,25}.

The presence of mycotoxins in food and feed has been investigated extensively. But few studies reported the occurrence of mycotoxins in surface, ground and wastewaters due to contamination from agricultural fields^{26,27}. Paterson et al., in 1997 first detected the presence of aflatoxins in cold storage water tank²⁸. Aflatoxin B₂ was the most often detected mycotoxin present in bottled water followed by aflatoxin B₁, aflatoxin G₁ and ochratoxin A²⁹. Even though, the levels of aflatoxins found in water is low (ng/L), long term exposure may cause health risk. Until now, no reports are available on UV degradation of aflatoxins in pure water. AFB₁ and AFM₁ have absorption maxima at 362 nm which elevate their susceptibility for degradation when exposed to light around 362 nm³⁰. Hence, we hypothesize irradiation of aflatoxins using UV-A light at 365 nm could be efficient to degrade aflatoxins in water via photo irradiation. The key points related to application of UVA light in aflatoxin reduction and detoxification include the analysis of kinetics, quantum yield and understanding the cytotoxic behavior of AFB₁ and AFM₁ degradation products for liver cells. Furthermore, a major issue in many UV studies is that they do not account the absorbance of the test fluid^{22,23}; hence, the present study rectifies this problem by accounting for fluid optics, and corrections for UV fluence gradients.

In this study, a custom-built laboratory scale batch reactor using an UV-A LED source which emits at a peak wavelength of 365 nm was used. This study is carried out to determine the degradation kinetics and the possible degradation mechanism of AFB₁ and AFM₁ in a pure water, without the hindrance of other biomolecules which may result in UV-A attenuation. This study also assesses the cytotoxicity of UV-A treated samples which contain residual AFB₁ and AFM₁ and their degradation products in water using human hepatoma cell line (HepG2).

Material and methods

Chemicals and reagents. AFB₁ and AFM₁ were procured from LKT laboratories, Inc (St. Paul MN, USA). Human hepatoma cells (HepG2; ATCC HB-8065), Eagle's minimum Essential Medium (EMEM; ATCC 30-2003), and fetal bovine serum (FBS; ATCC 30-2020) was purchased from American Type Culture Collection (ATCC, Manassas, VA).

Preparation of Aflatoxins standards in ultrapure water. Aflatoxin standard solutions were prepared by dissolving AFB₁ and AFM₁ in methanol. Working solutions of AFB₁ and AFM₁ with initial concentrations of 1 $\mu\text{g}/\text{mL}$ and 2 $\mu\text{g}/\text{mL}$, respectively were prepared in ultrapure water before being exposed to UV-A irradiation. As methanol is found to be toxic to cells, for cytotoxicity studies, AFB₁ and AFM₁ were dissolved in DMSO, each with initial concentration of 25 $\mu\text{g}/\text{mL}$.

Light emitting diodes irradiation system. A UV-A LED (IRTRONIX, Torrance, CA, USA) which emits at a peak wavelength of 365 nm, mounted on top of a quasi-collimated bench scale reactor, was used to perform the irradiation experiments. Five mL of the test solution was dispensed in a 10 mL beaker and placed above the magnetic stirrer. The test solution was continuously stirred to ensure uniform dose distribution and cold water (4 °C) was continuously circulated to prevent increase in temperature during irradiation at higher doses. Central irradiance incident on the surface of the test solution was measured with the help of a high sensitivity spectrometer (QE Pro series, Ocean Optics, Dunedin, FL, USA). Average irradiance was calculated by taking into account the absorption of the test solution at 365 nm. The absorbance was determined using a double

beam Cary100 Spectrophotometer connected to a 6-inch single integrating sphere (Agilent Technology, Santa Clara, CA, USA). The volume-averaged irradiance was evaluated by incorporating corrections factors (reflection factor, petri factor, divergence factor, water factor) as per the standard method described by Bolton and Linden³¹. Average irradiance was divided by target UV-A dose to obtain specific exposure times. Total UV-A doses of 0, 300, 600, 900 and 1,200 mJ/cm² were delivered to AFB₁ and AFM₁ test solutions and each treatment was done in triplicates in a randomized order.

$$\text{Average fluence (mW/cm}^2\text{)} = \text{Incident fluence} \times \left(\frac{1 - 10^{-(a \times d)}}{\ln(10) \times a \times d} \right) \times \left(\frac{L}{L + D} \right) \quad (1)$$

$$\text{UV - A Dose (mJ/cm}^2\text{)} = \text{Average fluence} \times \text{Treatment time (s)} \quad (2)$$

where 'Incident fluence' is the incident irradiance at the surface of the liquid, 'a' is the absorption coefficient per cm at 365 nm, d is the depth of fluid in the beaker, and 'L' is the distance from center of lamp source to the lower meniscus of the surface of the liquid.

HPLC analysis of AFB₁ and AFM₁. Separation and quantification of irradiated AFB₁, AFM₁ and their degradation products were carried out using a HPLC System (Shimadzu Scientific Instruments, Columbia, MD, USA) following the method described by Patras et al.¹⁶ with slight modification. A reversed-phase C₁₈ column (Phenomenex, CA, USA) with configuration 150 mm × 4.6 mm 2.6 μm, maintained at 37 °C was used as stationary phase. Separation was achieved with the mobile phase consisting of water/acetonitrile/methanol in the ratio of 120:75:30, under isocratic flow mode with a flow rate of 1 mL/min. Aflatoxins were detected using a Shimadzu RF-20A fluorescence detector with the excitation and emission wavelengths set at 365 and 450 nm respectively. The calibrated concentration for the HPLC method validation of AFB₁ and AFM₁ ranged between 0.25 and 1.0 μg/mL, 0.5 and 2.0 μg/mL for AFB₁ and AFM₁, respectively.

Aflatoxins degradation analysis LC-MS/MS. The identification of Aflatoxin B₁, M₁ and the respective degraded products was carried out with an LCMS method using a Shimadzu Prominence XR UHPLC system connected to a Shimadzu LCMS 8040 triple-stage quadrupole mass spectrometer with a chromatographic and mass spectrometric method described previously¹⁶. The column used for separation was a Phenomenex Kinetex 2.6 C18 column (50 × 2.1 mm, 2.6 μm). The injection volume was 5 μL. Control and experimental samples were injected, and data acquired in the scan mode to search for degraded products. Once degraded products were identified, corresponding selected ion monitoring (SIM) MS methods were developed for monitoring the parent and degraded product ions: AFB₁ (*m/z* 313), AFB₁ degraded products (*m/z* 303 and *m/z* 331), AFM₁ (*m/z* 329), and AFM₁ degraded products (*m/z* 347). The dwell time was 10 ms for all SIM events. Control and experimental samples were injected and analyzed. The chromatographic peak areas were determined and compared to controls with Shimadzu LabSolutions V5.89 software (Shimadzu, Columbia, MD, USA).

Cell cytotoxicity analysis. Cell cytotoxicity analysis was carried out using the method described by Patras et al.¹⁶ with slight modification. The HepG2 cells (American Type Culture Collection (ATCC); HB-8065) with a cell plating density of 2 × 10⁵ cells per well were seeded in a 12-well plate containing 10% (v/v) fetal bovine serum (FBS) in Eagle's minimal essential medium (EMEM). After 24 h, the cells were washed thrice with PBS and serum starved overnight in EMEM containing 1% FBS. Following serum starvation, the cells containing 1 mL media were exposed to 10% (v/v) of untreated and treated AFB₁ and AFM₁ test solutions at a final concentration of 2.5 μg/mL. After 48 h, the cells were measured for viability using XTT assay (ATCC, Manassas, VA) as per the manufacturer's protocol.

Kinetic modelling and data analysis. Log-linear reduction model available in the GInaFiT tool (a free-ware add-in for Microsoft Excel)³² was used to describe the UV-A degradation kinetics of aflatoxins (B₁ and M₁). This model provides good fit to data in which the inactivation exhibits first order kinetics and goodness of fit parameters including R², root mean square error, and rate constants were evaluated. The model is given in the following equation,

$$C = C_0 e^{-k_{max} \times D} \quad (3)$$

where 'C' is the initial concentration of aflatoxin, 'C₀' is the concentration of aflatoxin at dose D, 'k' is the degradation rate constant and D is the UV-A dose delivered.

For identification purposes, the expression was reformulated as,

$$\log_{10}(C) = \log_{10}(C_0) - \frac{k_{max} \times D}{\ln_{10}} \quad (4)$$

A balanced design with three replicates for each treatment was exposed to the selected UV-A treatment. Each sample was independent and assigned randomly to a treatment. One-way ANOVA with Tukey's HSD multiple comparison tests were performed to assess the effects of UV-A in SAS statistical computing environment (SAS, 2016). Data are presented as means ± standard deviation from the mean. Statistical significance was tested at 5 percent significance level.

Parameters	Aflatoxin B ₁	Aflatoxin M ₁
Irradiance (mW/cm ²)	10.26	10.26
Absorbance (Au/cm)	0.094	0.101
Transmittance (%T/cm)	80.5	79.250
Exposure time (s)	39, 78, 117, 156	39, 79, 118, 157
Delivered dose (mJ/cm ²)	300, 600, 900, 1,200	300, 600, 900, 1,200

Table 1. Optical properties and treatment parameters of AFB₁ and AFM₁ in ultrapure water under UV-A radiation.

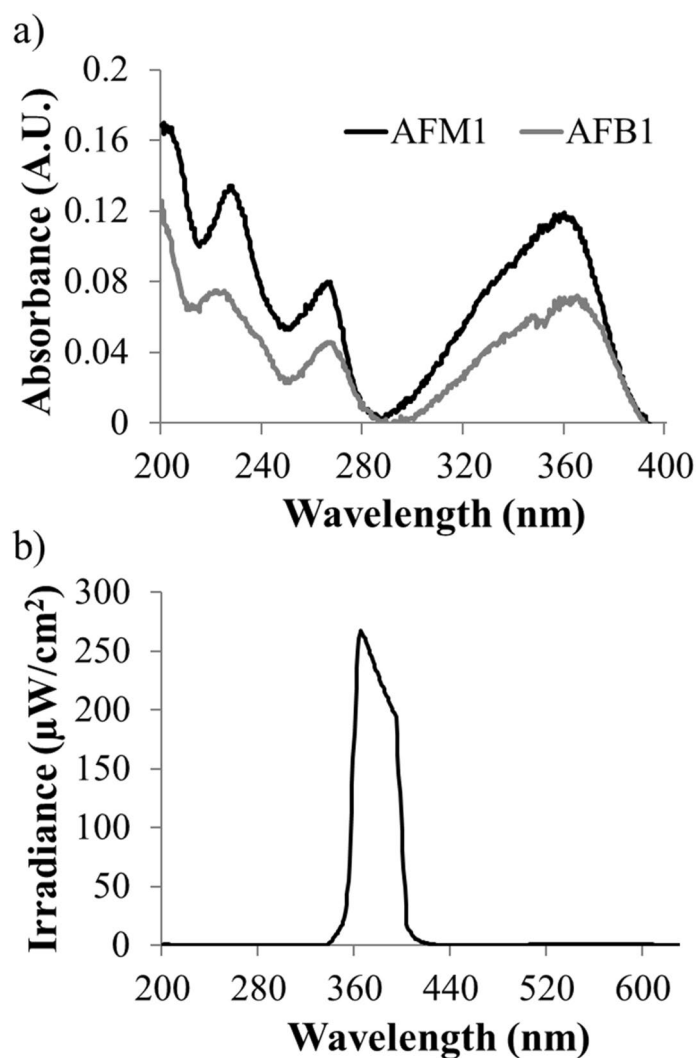


Figure 1. (a) Measured absorption spectra of AFB₁ and AFM₁ in ultrapure water using Cary100 spectrophotometer (b) Measured spectral irradiance of UV-A LED using Ocean optics QE Pro spectrometer equipped with UV-visible optical fiber.

Results and discussion

In this study, a novel UV-A LED which emits with the peak wavelength of 365 nm was used. The UV-A LED system employed in this study emits peak irradiance at 365 nm. Table 1 shows the characteristics (optical properties) of the test solutions prior to UV-A irradiation. The absorbance of AFB₁ and AFM₁ were 0.094 and 0.101/cm and ultraviolet transmittance (%) was calculated as 80.5 and 79.3/cm.

The absorption spectrum of AFB₁ and AFM₁ observed in the ultraviolet region of the electromagnetic spectrum and the relative emission spectra of the lamp are shown in Fig. 1. The data show AFB₁ and AFM₁ strongly

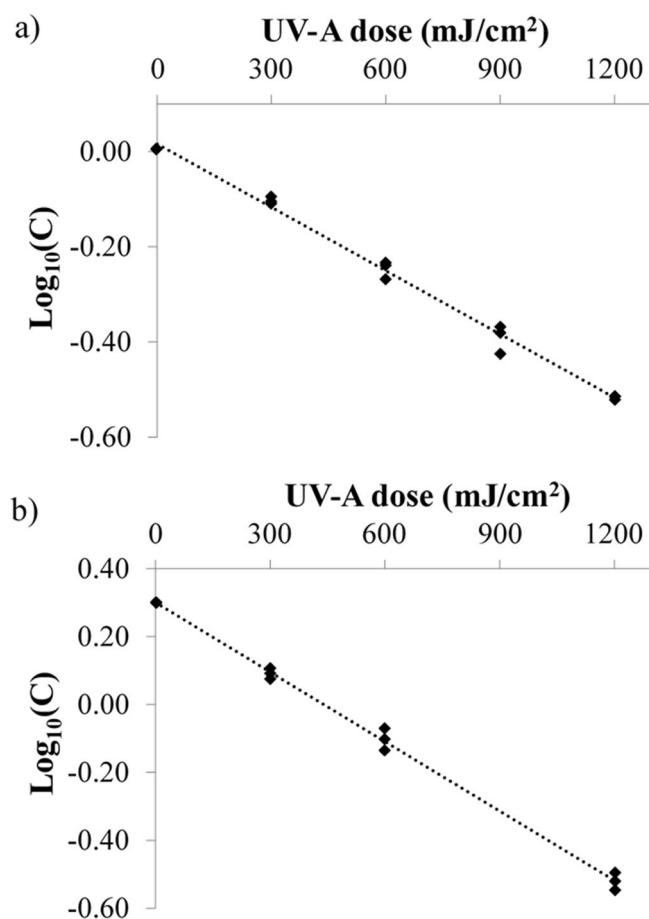


Figure 2. Degradation kinetics of (a) AFB₁ (b) AFM₁ in ultrapure water at different UV-A dose levels.

Parameters	Aflatoxin B ₁	Aflatoxin M ₁
R ²	0.99	0.99
K _{max} (cm ² /mJ)	0.001	0.0016
Half-life (mJ/cm ²)	693	433
Quantum yield	0.0043	0.0057

Table 2. Kinetic parameters of AFB₁ and AFM₁ under UV-A irradiation.

absorbs UV-A irradiation at 362 nm (Fig. 1a). The peak emission of the UV-A light source was noticed at 365 nm (Fig. 1b).

UV-A degradation kinetics of AFB₁ and AFM₁. In this study, Aflatoxins solutions AFB₁ and AFM₁ in ultrapure water were irradiated at different UV-A doses ranging from 0 to 1,200 mJ/cm². UV-A degradation of AFB₁ (C₀ = 0.997 ppm) and AFM₁ (C₀ = 2 ppm) in ultrapure water are compared in Fig. 2.

The degradation reaction followed first-order kinetics for AFB₁ and AFM₁ and both were reduced by more than 70%. At UV-A doses of 300, 600, 900 and 1,200 mJ/cm² AFB₁ reduced by 22.0 ± 1.32, 43.9 ± 2.34, 59.6 ± 2.66 and 70.0 ± 0.27 percent respectively. Similarly, a reduction of 36.0 ± 2.70, 57.5 ± 4.10, 76.3 ± 0.90, 84.0 ± 1.95 percent of AFM₁ was observed at UV-A doses 300, 600, 900 and 1,200 mJ/cm² respectively. Log₁₀(C) is plotted against the UV-A doses delivered. Table 2 shows the kinetic parameters of the irradiation experiment. Log linear trend was observed which indicates that the degradation of AFB₁ and AFM₁ in ultrapure water under UV-A irradiation follows first-order kinetics (R² > 0.99), given by the Eq. (4). The kinetic rate constant for AFB₁ degradation in water was 0.001 cm²/mJ, which is ~ 1.6 times lesser than the kinetic constants for AFM₁ (0.0016 cm²/mJ).

Quantum yield is a fundamental photochemical parameter, which explains the photochemical fate of the compound, under controlled conditions where light absorption and change in target compound concentration

UV-A dose (mJ/cm ²)	Irradiance (W/m ²)	Treatment time (s)	Absorbed energy (J/m ³)	Einsteins absorbed (E/m ³)	Aflatoxin (mol/m ³)	Quantum yield
AFB₁						
300	102.6	39	79,236	0.24	0.0025	0.0105
600	102.6	78	158,473	0.48	0.0018	0.0038
900	102.6	117	237,709	0.73	0.0013	0.0018
1,200	102.6	156	316,945	0.97	0.0010	0.0010
					Average	0.0043
AFM₁						
300	102.6	39	84,171	0.26	0.0032	0.0039
600	102.6	79	170,500	0.52	0.0022	0.0026
900	102.6	118	254,671	0.78	0.0014	0.0014
1,200	102.6	157	338,842	1.03	0.0010	0.0010
					Average	0.0057

Table 3. Quantum yield calculation of AFB₁ and AFM₁ in ultrapure water under UV-A radiation.

are properly quantified^{33,34}. Quantum yield is the number of defined events occurring per photon absorbed by the system³⁵. For a photochemical reaction, quantum yield $\phi(\lambda)$ at a wavelength λ is given by,

$$\phi(\lambda) = \frac{\text{moles of reactant consumed or products formed}}{\text{Einsteins absorbed}} \quad (5)$$

Einsteins absorbed during the UV-A treatment is easily obtained by the following equation; The energy of a single photon is quantified by the following law:

$$E = \frac{hc}{\lambda} \quad (6)$$

where h = Planck constant (6.63×10^{-34} J s), c = light speed (3×10^8 m/s), λ = wavelength (m). In our case

$$E = \frac{6.63 \times 10^{-34} [\text{J s}] \times 3 \times 10^8 \left[\frac{\text{m}}{\text{s}}\right]}{3.65 \times 10^{-7} \text{ m}} = 5.44222E - 19 \text{ J} \quad (7)$$

Absorbed energy is given by:

$$\text{Einsteins absorbed (E m}^3) = \frac{(\text{Absorbed energy/Photon energy at 365 nm})}{\text{energy in 1 mole of photons}} \quad (8)$$

$$\text{Absorbed energy (J m}^3) = \left(\frac{\text{Power absorbed} \times \text{treatment time(s)}}{\text{Volume (m}^3)} \right) \quad (9)$$

Power absorbed is obtained by following equation:

$$\text{Power absorbed (W/s)} = (I_0) \times (A) - I_0(A)10^{-(A_{365} \times d)} \quad (10)$$

where I_0 is surface irradiance (W/m²); A is the area (m²), A_{365} is the absorbance value at 365 nm (base10/m), d is the fluid depth (m).

The quantum yields of AFB₁ and AFM₁ in ultrapure water were determined based on Table 3.

The average quantum yields of AFB₁ and AFM₁ in ultrapure water were found to be 4.25×10^{-3} and 5.74×10^{-3} respectively. The quantum yield of AFM₁ in ultrapure water is 1.35 times more than that of the quantum yield of AFB₁. Comparing the UV-A photolysis rate constants, and quantum yield, it is found that AFM₁ is more susceptible to UV-A photolysis than AFB₁.

Under UV-A radiation, AFB₁ acts as a photosensitizer and results in the formation of reactive oxygen species through the involvement of triplet excited state, by either Type I or Type II mechanism. In Type I mechanism, electron transfer occurs from triplet aflatoxin to molecular oxygen resulting in the formation of superoxide anion radical. In Type II mechanism, energy is transferred from triplet aflatoxin to molecular oxygen leading to singlet oxygen formation. These reactive species react with the aflatoxins and form oxidized products³⁶. Various authors have studied the degradation kinetics of aflatoxins. For example, Patras et al. observed 98% reduction of AFB₁ with a UV dose of 4,880 mJ/cm² in ultrapure water when irradiated using medium pressure lamp which emits irradiation between 220 and 400 nm¹⁶. Similarly, Liu et al. used UV lamp emitting at 220–400 nm with an irradiance of 800 μW/cm² and observed thorough reduction of AFB₁ in peanut oil after 30 min of UV exposure, the degradation followed first order kinetics²². Mao et al. used a UV-A lamp (lamp power = 100 W; irradiance = 55–60 mW cm²) which emits at 365 nm to treat AFB₁ in peanut oil, the authors observed ≈96% reduction after 30 min of UV-A exposure (UV dose equivalent = 108,000 mJ/cm²)³⁷. Diao et al. tested a continuous flow UV-A reactor

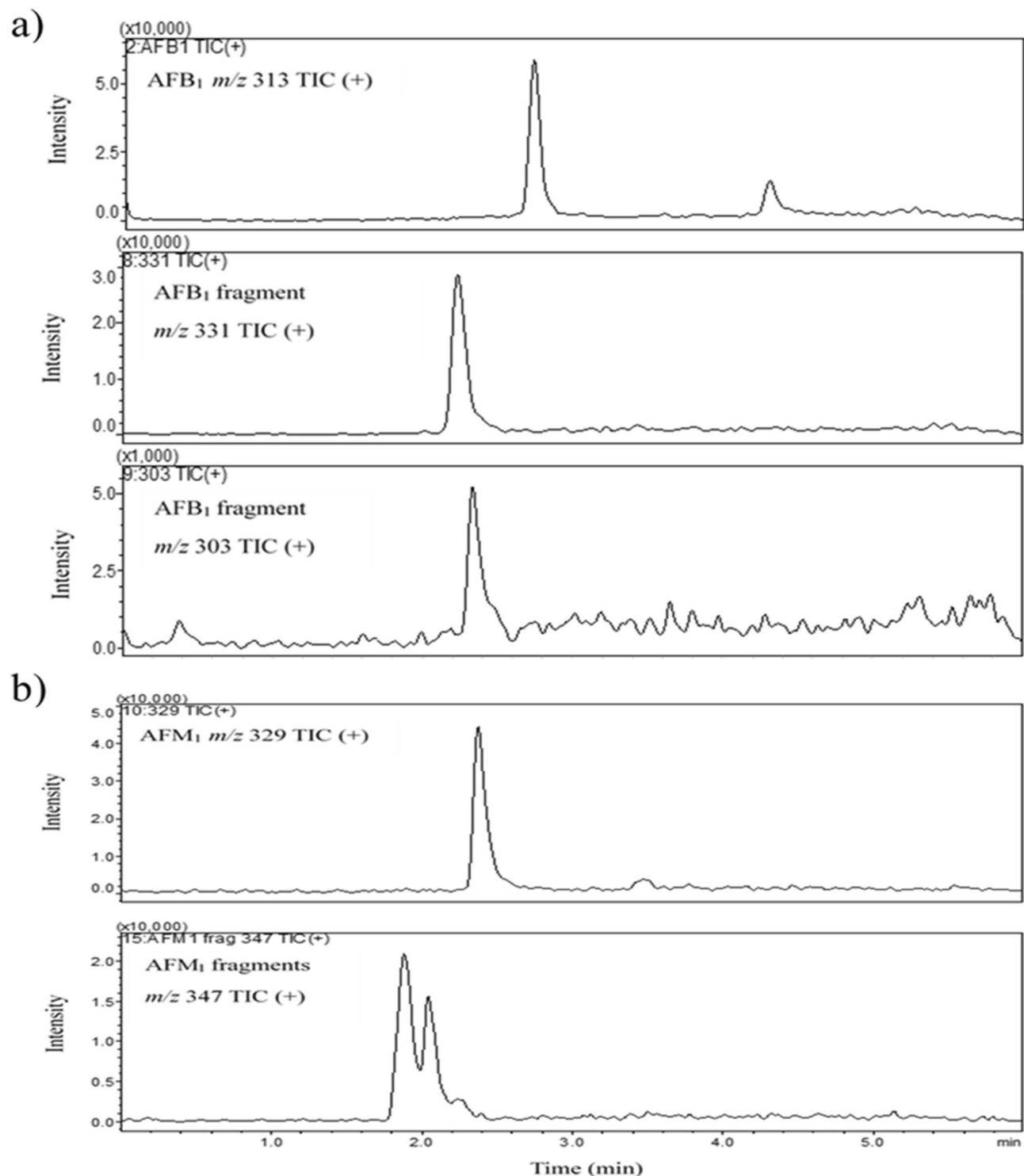


Figure 3. LCMS single ion monitoring (SIM) total ion chromatograms (TIC) of (a) AFB₁ and (b) AFM₁ samples treated at UV-A dose 1,200 mJ/cm².

(lamp power = 36 W; irradiance = 6.4 mW/cm²; flow rate = 0.55 L/min) to treat AFB₁ in peanut oil at 365 nm and observed 88.74% reduction after 40 min of UV-A exposure³⁸. It should be noted that the authors did not report the UV-A doses; a common discrepancy in many studies. From the above studies, it is quite evident that optical based techniques (i.e. irradiation) can degrade the aflatoxins efficiently due to their photosensitivity.

AFB₁ and AFM₁ degradation products. LC-MS scans were used to search for degraded products of AFB₁ and AFM₁ in water after UV-A irradiation, and are given in Fig. 3.

LC–MS single ion monitoring (SIM) chromatographic peaks were analyzed as a qualitative approach to approximate the amount of degraded products produced by determining the areas of (SIM) chromatographic peaks. Since authentic standards of the degraded products are not readily available, a quantitative approach is not possible. When compared to controls, LC–MS peak areas for AFB₁ and AFM₁ decreased and the peak areas of the degraded products increased significantly with increase in the UV-A dose. Representative SIM chromatograms and the LC–MS peak areas for AFB₁ and AFM₁ are presented in the supplemental information (Figure S1).

The structure of the degraded products of AFB₁ and AFM₁ was identified and the possible degradation pathway is proposed based on them, as given by Fig. 4. Two degradation products, P₁ and P₂ were observed for AFB₁ in water. Hydration and demethoxylation were the main fragmentation pathways of AFB₁. The double bond equivalence (DBE) of AFB₁ is 12. The photolysis product C₁₇H₁₄O₇ (P₁, *m/z* 331.08) was the result of hydration on the double bond of terminal furan ring of AFB₁, with DBE of 11 which is one less than AFB₁. The structure of product C₁₇H₁₄O₇ (P₁, *m/z* 331.08) is similar to that of Aflatoxin B_{2A}, whose toxic potential is comparatively less than AFB₁, and is inactive with respect to toxicity to ducklings and is non-lethal to chick embryos^{39,40}. Product C₁₆H₁₄O₆ (P₂) (*m/z* 303) was the result of hydration on furan ring and demethylation on the side chain of benzene. The DBE of P₂ is 10, which is 2 less than AFB₁. The AFB₁ degraded products had retention times of 2.2 and 2.3 min.

Two degraded products with similar chemical formula C₁₇H₁₄O₈ (*m/z* 347.07) were observed for AFM₁ and were found to be structural isomers of each other. Hydration was observed to be the main fragmentation pathway which occurred at the double bond of terminal furan ring. The DBE of both the products were found to be 11, which is one less than AFM₁ (DBE of AFM₁ = 12). The AFM₁ degraded products had retention times of 1.8 and 2.0 min. The DBE of all the photolysis products of both AFB₁ and AFM₁ were found to be less than that of their parent molecules, implying that double bond addition reactions occurred.

The UV-A irradiation results in the formation of reactive species, which react with AFB₁ and AFM₁ resulting in photolysis. Hence, the structure of all photolysis products formed due to the reaction of free radicals with AFB₁ and AFM₁ is almost similar to that of their parent molecules⁴¹. The double bond in the terminal furan ring and the lactone ring in the coumarin moiety are considered to be the most toxicological sites of AFB₁⁴². While AFB₁ is not mutagenic, it is bioactivated by undergoing epoxidation of double bond in the furan ring results in the formation of AFB₁-8,9-epoxide and it is the key active site for its toxic and carcinogenic activities as the aflatoxin-DNA and the aflatoxin-protein interactions occur^{6,7}. From the proposed structure of the degradation products, it is shown that the double bond in the terminal furan ring is removed in the degradation products of both AFB₁ and AFM₁. Hence, based on quantitative structure–activity relationships, it is evident that the toxicity of the photolysis products is reduced compared to the toxicity of AFB₁ and AFM₁.

Cytotoxicity analysis. Aflatoxins are reported to reduce cell survival in various cultured cells, especially HepG2 cells as liver is the target organ of aflatoxins^{43,44}. Several literature studies have demonstrated aflatoxins-induced oxidative stress damage, and its effect in hepatotoxicity^{45–47}. AFB₁ can induce reactive oxygen species (ROS) to cause oxidative stress, also cause genetic alterations prone to DNA damage and alter mitochondrial permeability^{46,48,49}. Liu et al. (2016) reported precise mechanism of AFB₁ induced on hepatotoxicity in primary broiler hepatocytes, AFB₁ impaired mitochondrial functions by inducing reactive oxygen species and oxidative stress resulting in the activation of caspase-3 and caspase-9-induced apoptosis through mitochondrial signal pathway in addition to maintaining proper redox balance⁵⁰. On the other hand, AFM₁ is a detoxification product of AFB₁, and AFM₁ showed only 10% of mutagenicity when compared to AFB₁⁵¹. The metabolic fate of AFM₁ resulted to be similar to that of AFB₁, with the difference that AFM₁ represents a poorer substrate for epoxidation, thus explaining the differences in genotoxicity potencies. Moreover, it has been reported that Cytochrome P450 (CYP) activation is not required to AFM₁ to exert cytotoxic effects⁵².

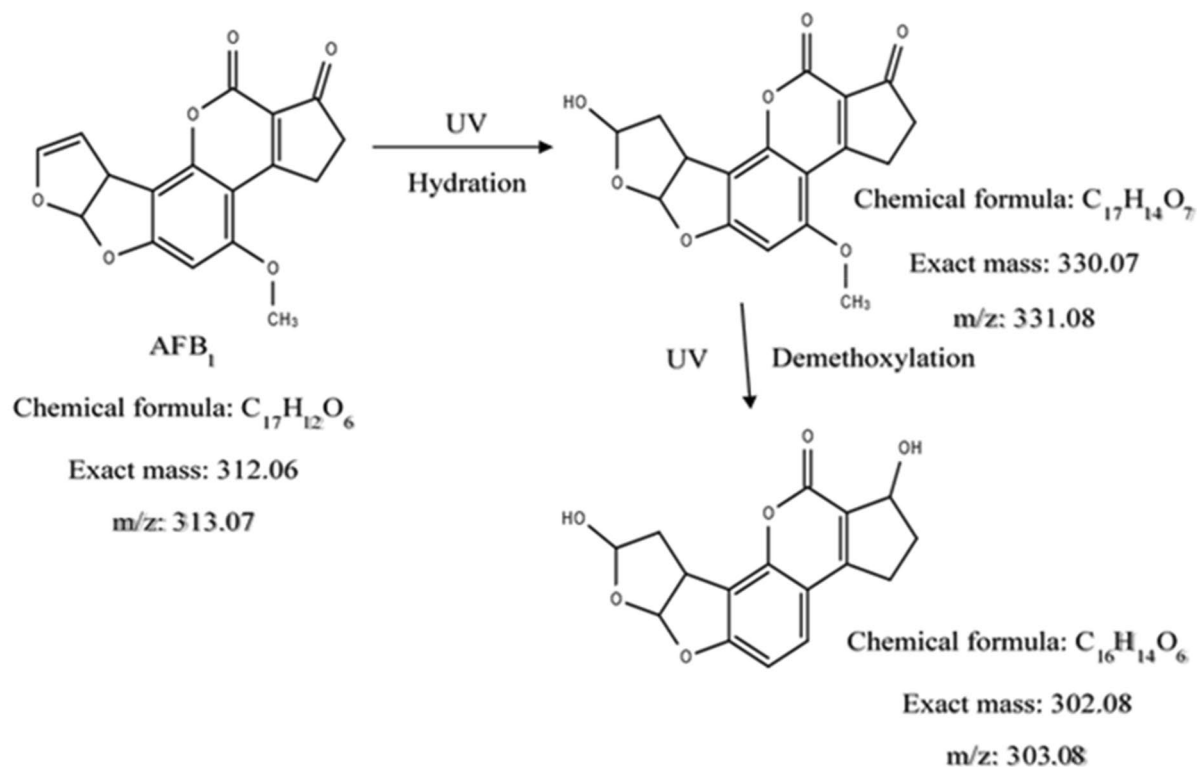
The efficiency of the UV treatment in reducing the toxic potential of AFB₁ and AFM₁ was studied using in vitro cell culture methods. The cell viability was assessed using XTT [2,3-bis-(2-methoxy-4-nitro-5-sulphophenyl)-2H-tetrazolium-5-carboxanilide] assay, and the results were given in Fig. 5.

The cells were exposed to the test samples for 48 h. With an increase in the UV-A dose from 0 to 1,200 mJ/cm², the cell viabilities increased from 52.5 ± 1.1 to 101.1 ± 3.2% in the samples treated with AFB₁ respectively. Similarly, when the UV-A dose increased from 0 to 1,200 mJ/cm², the cell viabilities increased from 70.42 ± 5.25 to 98.44 ± 0.25% in the samples treated with AFM₁ respectively. The difference in cell viability between the treated and the control samples were found to be statistically significant. As the doses increased from 0 to 1,200 mJ/cm², there is a significant decrease in the concentration of AFB₁ (p value 0.001) and AFM₁ (p value 0.0027), and thereby increase in cell viabilities was observed. Also, it is worth mentioning that there is no significant difference between the negative control and the maximum applied dose of 1,200 mJ/cm² for both AFB₁ (p value 0.76) and AFM₁ (p value 0.899), clearly demonstrating the efficiency of UV-A degradation.

Conclusion

The current research clearly demonstrated the efficiency of UV-A light in photolysis of AFB₁ and AFM₁ in ultrapure water. The results show that AFB₁ and AFM₁ were significantly reduced with increase in UV-A dose. A reduction of 70% and 84% were observed at 1,200 mJ/cm² respectively. Likewise, cytotoxicity analysis of UV-A treated samples using HepG2 liver cells show increase in cell viability as the dose increases from 0 to 1,200 mJ/cm² and no cytotoxicity was observed at UV-A dose of 1,200 mJ/cm². These results confirm that the degraded AFB₁ and AFM₁ products of UV-A photolysis in water are safe without any effect on cell viability. Overall the results revealed that efficient degradation of AFB₁ and AFM₁ using UV-A irradiation at 365 nm could be a potential approach to reduce their levels in contaminated water. Due to its lipophilic nature, milk and edible vegetable oils are typically contaminated by aflatoxins hence could be reduced by UV-A light. Further studies will be conducted

a)



b)

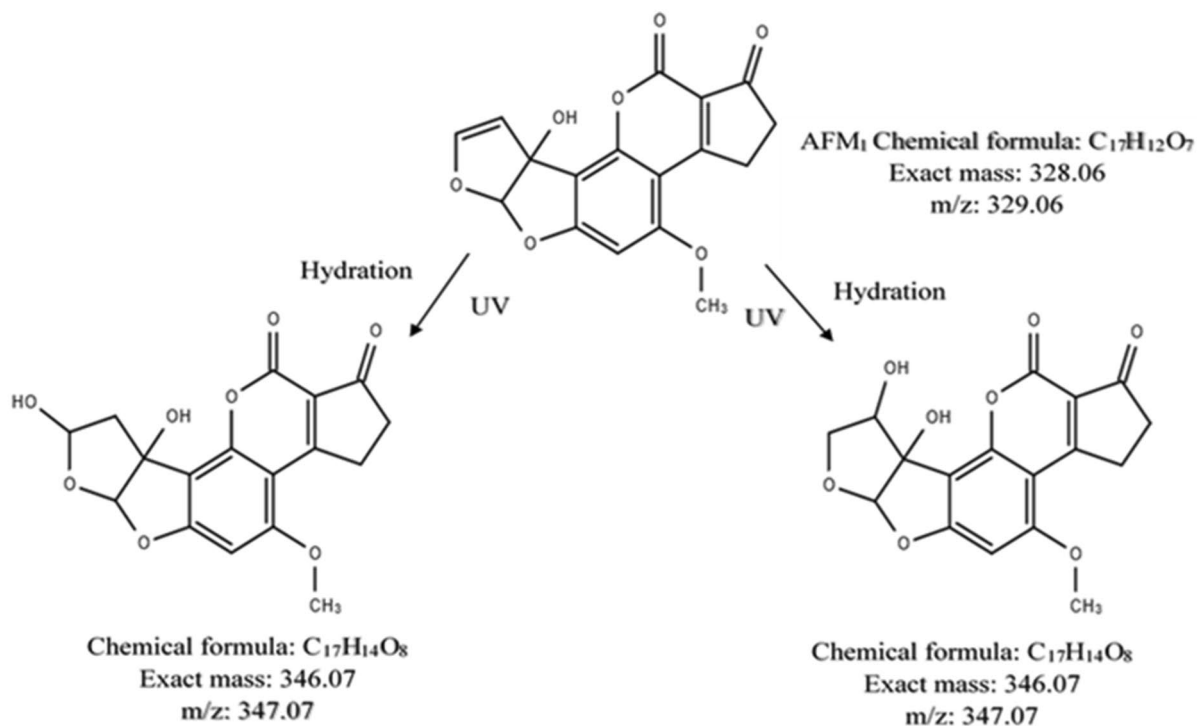


Figure 4. Proposed UV-A light degradation mechanism of (a) AFB₁ and (b) AFM₁ in ultrapure water.

to assess the efficiency of this technology on reduction of AFB₁ and AFM₁ levels, quality (nutritional and sensory) and safety of the food products (milk and edible vegetable oils). Since AFB₁ and AFM₁ have absorbance maxima at 365 nm and milk and edible vegetable oils have absorbance minima at 365 nm, this permits efficient degradation of AFB₁ and AFM₁ by improving light penetration while potentially having less impact on the nutritional and sensory quality of food. UV-A dose response curves of aflatoxins will be generated using a continuous flow UV system, continuous flow reactors are significantly more desirable for industrial food processes.

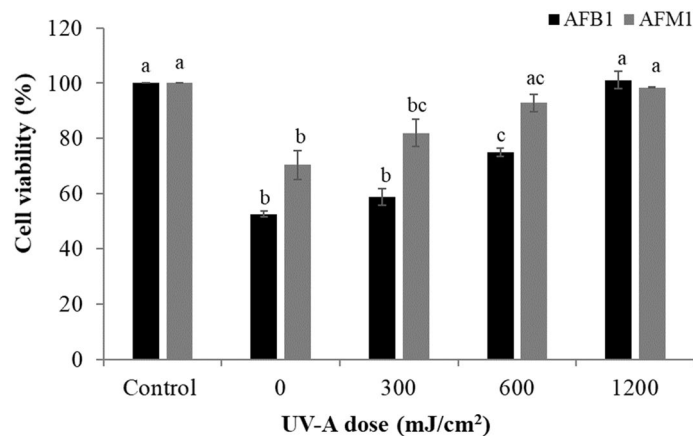


Figure 5. Cytotoxic effect of untreated and UV-A treated ultrapure water consists of (a) AFB₁, (b) AFM₁ on human hepatoma HepG2 cells. Results are expressed as mean percentage \pm SD of two separate experiments. Levels connected by different letters are significantly different at $p < 0.05$.

Received: 1 January 2020; Accepted: 22 May 2020

Published online: 10 August 2020

References

- Pankaj, S. K., Shi, H. & Keener, K. M. A review of novel physical and chemical decontamination technologies for aflatoxin in food. *Trends Food Sci. Technol.* **71**, 73–83 (2018).
- Asao, T. *et al.* The structures of aflatoxins B and G₁. *J. Am. Chem. Soc.* **87**, 882–886 (1965).
- Rustum, I. Y. S. *Aflatoxin in Food and Feed: Occurrence, Legislation and Inactivation by Physical Methods*. Food Chemistry Vol. 59 (Elsevier, Amsterdam, 1997).
- Dhanasekaran, D., Shanmugapriya, S., Thajuddin, N. & Panneerselvam, A. Aflatoxins and aflatoxicosis in human and animals. *Aflatoxins Biochem. Mol. Biol.* <https://doi.org/10.5772/22717> (2011).
- Kamkar, A., Fallah, A. A. & Mozaffari Nejad, A. S. The review of aflatoxin M₁ contamination in milk and dairy products produced in Iran. *Toxin Rev.* **33**, 160–168 (2014).
- Marin, S., Ramos, A. J., Cano-Sancho, G. & Sanchis, V. Mycotoxins: occurrence, toxicology, and exposure assessment. *Food Chem. Toxicol.* **60**, 218–237 (2013).
- Samarajeeva, U., Sen, A. C., Cohen, M. D. & Wei, C. I. Detoxification of aflatoxins in foods and feeds by physical and chemical methods. *J. Food Prot.* **53**, 489–501 (1990).
- International Agency for Research on Cancer (IARC). Some naturally occurring substances: food items and constituents, heterocyclic aromatic amines and mycotoxins. in *Aflatoxins 245–295* (1993).
- Udomkun, P. *et al.* Innovative technologies to manage aflatoxins in foods and feeds and the profitability of application—a review. *Food Control* **76**, 127–138 (2017).
- Iqbal, S. Z., Jinap, S., Pirouz, A. A. & Ahmad Faizal, A. R. Aflatoxin M₁ in milk and dairy products, occurrence and recent challenges: a review. *Trends Food Sci. Technol.* **46**, 110–119 (2015).
- Guo, W. *et al.* Reduced graphene oxide-gold nanoparticle nanoframework as a highly selective separation material for aflatoxins. *Sci. Rep.* <https://doi.org/10.1038/s41598-017-15210-1> (2017).
- Iram, W., Anjum, T., Iqbal, M., Ghaffar, A. & Abbas, M. Mass spectrometric identification and toxicity assessment of degraded products of aflatoxin B₁ and B₂ by *Corymbia citriodora* aqueous extracts. *Sci. Rep.* **5**, 14672 (2015).
- Prietto, L. *et al.* Post-harvest operations and aflatoxin levels in rice (*Oryza sativa*). *Crop Prot.* **78**, 172–177 (2015).
- Wang, B. *et al.* Effectiveness of pulsed light treatment for degradation and detoxification of aflatoxin B₁ and B₂ in rough rice and rice bran. *Food Control* **59**, 461–467 (2016).
- Moreau, M. *et al.* Application of the pulsed light technology to mycotoxin degradation and inactivation. *J. Appl. Toxicol.* **33**, 357–363 (2013).
- Patras, A. *et al.* Effect of UV irradiation on aflatoxin reduction: a cytotoxicity evaluation study using human hepatoma cell line. *Mycotoxin Res.* **33**, 343–350 (2017).
- Chandra, S. *et al.* Patulin degradation and cytotoxicity evaluation of UV irradiated apple juice using human peripheral blood mononuclear cells. *J. Food Process Eng.* **40**, 1–9 (2017).
- Gopisetty, V. V. S. *et al.* Impact of UV-C irradiation on the quality, safety, and cytotoxicity of cranberry-flavored water using a novel continuous flow UV system. *LWT* **95**, 230–239 (2018).
- Pendyala, B., Patras, A., Gopisetty, V. V. S., Sages, M. & Balamurugan, S. Inactivation of bacillus and clostridium spores in coconut water by ultraviolet light. *Foodborne Pathog. Dis.* **16**, 704–711 (2019).
- Pendyala, B., Patras, A., Ramaswamy, R., Gopisetty, V. V. S. & Sages, M. Evaluation of UV-C irradiation treatments on microbial safety, ascorbic acid, and volatile aromatics content of watermelon beverage. *Food Bioprocess. Technol.* <https://doi.org/10.1007/s11947-019-02363-2> (2019).
- Van der Zijden, A. S. M. *et al.* Aspergillus flavus and Turkey X disease: isolation in crystalline form of a toxin responsible for Turkey X disease. *Nat. Int. J. Sci.* **196**, 1048–1050 (1962).
- Liu, R. *et al.* Photodegradation of aflatoxin B₁ in peanut oil. *Eur. Food Res. Technol.* **232**, 843–849 (2011).
- Yousef, A. E. & Marth, E. H. Degradation of aflatoxin M₁ in milk by ultraviolet energy. *J. Food Prot.* **48**, 697–698 (1985).
- Koutchma, T. Advances in ultraviolet light technology for non-thermal processing of liquid foods. *Food Bioprocess. Technol.* **2**, 138–155 (2009).

25. Antonio-Gutiérrez, O. T., López-Díaz, A. S., López-Malo, A., Palou, E. & Ramírez-Corona, N. *UV-C Light for Processing Beverages: Principles, Applications, and Future Trends. Processing and Sustainability of Beverages* (Elsevier, 2019). <https://doi.org/10.1016/b978-0-12-815259-1.00007-0>.
26. Gromadzka, K., Waśkiewicz, A., Goliński, P. & Świetlik, J. Occurrence of estrogenic mycotoxin—Zearalenone in aqueous environmental samples with various NOM content. *Water Res.* <https://doi.org/10.1016/j.watres.2008.11.042> (2009).
27. Laganà, A. *et al.* Analytical methodologies for determining the occurrence of endocrine disrupting chemicals in sewage treatment plants and natural waters. *Anal. Chim. Acta* <https://doi.org/10.1016/j.aca.2003.09.020> (2004).
28. Paterson, R. R. M., Kelley, J. & Gallagher, M. Natural occurrence of aflatoxins and *Aspergillus flavus* (Link) in water. *Letts. Appl. Microbiol.* <https://doi.org/10.1111/j.1472-765X.1997.tb00012.x> (1997).
29. Mata, A. T. *et al.* Bottled water: analysis of mycotoxins by LC-MS/MS. *Food Chem.* <https://doi.org/10.1016/j.foodchem.2014.12.088> (2015).
30. Jubeen, F., Bhatti, I. A., Khan, M. Z., Zahoor-Ul-Hassan, H. & Shahid, M. Effect of UVC irradiation on aflatoxins in ground nut (*Arachis hypogea*) and tree nuts (*Juglans regia*, *prunus dulcis* and *pistachio vera*). *J. Chem. Soc. Pak.* **34**, 1366–1374 (2012).
31. Bolton, J. R. & Linden, K. G. Standardization of methods for fluence (UV dose) determination in bench-scale UV experiments. *J. Environ. Eng.* **129**, 209–215 (2003).
32. Geeraerd, A. H., Valdramidis, V. P. & Van Impe, J. F. GInaFIT, a freeware tool to assess non-log-linear microbial survivor curves. *Int. J. Food Microbiol.* **102**, 95–105 (2005).
33. Reina, A. C. *et al.* Photochemical degradation of the carbapenem antibiotics imipenem and meropenem in aqueous solutions under solar radiation. *Water Res.* **128**, 61–70 (2018).
34. Challis, J. K., Hanson, M. L., Friesen, K. J. & Wong, C. S. A critical assessment of the photodegradation of pharmaceuticals in aquatic environments: defining our current understanding and identifying knowledge gaps. *Environ. Sci. Process. Impacts* **16**, 672–696 (2014).
35. Bolton, J. R., Mayor-Smith, I. & Linden, K. G. Rethinking the concepts of fluence (UV dose) and fluence rate: the importance of photon-based units—a systemic review. *Photochem. Photobiol.* **91**, 1252–1262 (2015).
36. Netto-Ferreira, J. C., Heyne, B. & Scaiano, J. C. Photophysics and photochemistry of aflatoxins B1 and B2. *Photochem. Photobiol. Sci.* **10**, 1701–1708 (2011).
37. Mao, J. *et al.* A structure identification and toxicity assessment of the degradation products of aflatoxin B1 in peanut oil under UV irradiation. *Toxins (Basel)* **8**, 332 (2016).
38. Diao, E. *et al.* Safety evaluation of aflatoxin B1 in peanut oil after ultraviolet irradiation detoxification in a photodegradation reactor. *Int. J. Food Sci. Technol.* **50**, 41–47 (2015).
39. Wogan, G. N., Edwards, G. S. & Newberne, P. M. Structure-activity relationships in toxicity and carcinogenicity of aflatoxins and analogs. *Cancer Res.* **31**, 1936–1942 (1971).
40. Lillehoj, E. B. & Ciegler, A. Biological activity of aflatoxin B2a. *Appl. Microbiol.* **17**, 516–519 (1969).
41. Wang, F. *et al.* Structure elucidation and toxicity analyses of the radiolytic products of aflatoxin B1 in methanol-water solution. *J. Hazard. Mater.* **192**, 1192–1202 (2011).
42. Lee, L. S., Dunn, J. J., DeLucca, A. J. & Ciegler, A. Role of lactone ring of aflatoxin B1 in toxicity and mutagenicity. *Experientia* **37**, 16–17 (1981).
43. Van Vleet, T. R., Watterson, T. L., Klein, P. J. & Coulombe, R. A. Aflatoxin B1 alters the expression of p53 in cytochrome p450-expressing human lung cells. *Toxicol. Sci.* **89**, 399–407 (2006).
44. Liu, Y., Du, M. & Zhang, G. Proapoptotic activity of aflatoxin B1 and sterigmatocystin in HepG2 cells. *Toxicol. Rep.* **1**, 1076–1086 (2014).
45. Yener, Z., Celik, I., Ilhan, F. & Bal, R. Effects of *Urtica dioica* L. seed on lipid peroxidation, antioxidants and liver pathology in aflatoxin-induced tissue injury in rats. *Food Chem. Toxicol.* <https://doi.org/10.1016/j.fct.2008.11.031> (2009).
46. Shi, D. *et al.* Protective effects of selenium on aflatoxin B1-induced mitochondrial permeability transition, DNA damage, and histological alterations in duckling liver. *Biol. Trace Elem. Res.* <https://doi.org/10.1007/s12011-014-0189-z> (2015).
47. Shi, J. *et al.* Distinct response of the hepatic transcriptome to Aflatoxin B1 induced hepatocellular carcinogenesis and resistance in rats. *Sci. Rep.* <https://doi.org/10.1038/srep31898> (2016).
48. Theumer, M. G. *et al.* Subchronic mycotoxicoses in Wistar rats: assessment of the in vivo and in vitro genotoxicity induced by fumonisin and aflatoxin B1, and oxidative stress biomarkers status. *Toxicology* <https://doi.org/10.1016/j.tox.2009.12.007> (2010).
49. Mary, V. S., Theumer, M. G., Arias, S. L. & Rubinstein, H. R. Reactive oxygen species sources and biomolecular oxidative damage induced by aflatoxin B1 and fumonisin B1 in rat spleen mononuclear cells. *Toxicology* <https://doi.org/10.1016/j.tox.2012.08.012> (2012).
50. Liu, Y. & Wang, W. Aflatoxin B1 impairs mitochondrial functions, activates ROS generation, induces apoptosis and involves Nrf2 signal pathway in primary broiler hepatocytes. *Anim. Sci. J.* **87**, 1490–1500 (2016).
51. Wogan, G. N. & Paglialunga, S. Carcinogenicity of synthetic aflatoxin M1 in rats. *Food Cosmet. Toxicol.* [https://doi.org/10.1016/0015-6264\(74\)90012-1](https://doi.org/10.1016/0015-6264(74)90012-1) (1974).
52. Neal, G. E., Eaton, D. L., Judah, D. J. & Verma, A. Metabolism and toxicity of aflatoxins M1 and B1 in human-derived in vitro systems. *Toxicol. Appl. Pharmacol.* **151**, 152–158 (1998).

Acknowledgements

This project is funded under the Agriculture and Food Research Initiative (Food Safety Challenge Area), USDA, Award Numbers; 2015-69003-23117 and 2018-38821-27732. The authors would like to thank Ms. Judy Stanley for all her dedication and hardwork. She was a remarkable scientist. We will remember her forever.

Author contributions

Conceived and designed the experiments: J.S., A.P. and B.P. Performed the experiments: J.S., B.P., M.J.V., and R.R.B. Analyzed the data: J.S., A.P. B.P., M.J.V., and R.R.B. Wrote the paper: J.S. and B.P. Revised the paper: A.P., B.P., M.J.V., and R.R.B.

Competing interests

The authors declare no competing interests.

Additional information

Supplementary information is available for this paper at <https://doi.org/10.1038/s41598-020-70370-x>.

Correspondence and requests for materials should be addressed to A.P. or B.P.

Reprints and permissions information is available at www.nature.com/reprints.

Publisher's note Springer Nature remains neutral with regard to jurisdictional claims in published maps and institutional affiliations.



Open Access This article is licensed under a Creative Commons Attribution 4.0 International License, which permits use, sharing, adaptation, distribution and reproduction in any medium or format, as long as you give appropriate credit to the original author(s) and the source, provide a link to the Creative Commons license, and indicate if changes were made. The images or other third party material in this article are included in the article's Creative Commons license, unless indicated otherwise in a credit line to the material. If material is not included in the article's Creative Commons license and your intended use is not permitted by statutory regulation or exceeds the permitted use, you will need to obtain permission directly from the copyright holder. To view a copy of this license, visit <http://creativecommons.org/licenses/by/4.0/>.

© The Author(s) 2020